MMP-2 sensitive and reduction-responsive prodrug amphiphile for active targeted therapy of cancer by hierarchical cleavage

Xueni Zhang,[a] Lihui Dai,[a] Yumeng Ding,[a] Qian Liu,[a] Xiaoya Li,[a] Mengting Liu,[a] Meng Meng,[a] Jie Pan,[*b] Rimo Xi [*a] and Yongmei Yin [*a]

[a] State Key Laboratory of Medicinal Chemical Biology, College of Pharmacy, and Tianjin Key Laboratory of Molecular Drug Research, Nankai University, Haihe Education Park, 38 Tongyan Road, Tianjin 300353, China

[b] School of Chemical Engineering and Technology, Tiangong University, Tianjin 300387, China

Correspondence:
panjie@tiangong.edu.cn;
xirimo@nankai.edu.cn;
yinyongmei@nankai.edu.cn

1.Materials and methods

1.1 Materials

The peptide (GPLGVRGDG) was prepared according to the standard Fmoc protected solid-phase peptide synthesis (SPPS) method report [1-2]. All the solvents were purchased from Bohua Chemical Reagent Co., Ltd. (Tianjin, China). Camptothecin (CPT) was purchased from HEOWNS Co., Ltd. (Tianjin, China). mPEG-COOH (MW 3400 Da) was from Yanyi Biological Technology Co., Ltd. (Shanghai, China). Glutatione (GSH) was purchased from Aladdin Chemistry Co., Ltd. (Shanghai, China). MMP-2 enzyme was from CHI Scientific Co., Ltd. (Jiangsu, China). 3-(4,5-Dimethylthiazol-2-yl)-2,5-diphenyl tetrazolium bromide (MTT) was purchased from Solarbio Science & Technology Co., Ltd. (Beijing, China). RPMI 1640 medium, DMEM medium and fetal bovine serum were from Gibco (BRL, MD, USA). All the chemicals were used as received.

1.2 Cell Culture and Animals

Human nonsmall lung carcinoma cells (A549) and mouse mammary breast tumor cells (4T1) were cultured in RPMI 1640 medium, and human hepatoma cells (HepG2) were cultured in DMEM medium; all the mediums were mixed with 10% fetal bovine serum (FBS). All the cells were cultured at 37°C under humidified CO_2 atmosphere (5%). Female BALB/c mice (6-8 weeks) were purchased from Vital River Laboratory Animal Technology Co., Ltd. (Beijing, China). All animal experiments followed the institutional and national guidelines and were approved by the appropriate institutional review.

1.3 Synthesis of mPEG-GPLGVRGDG-COOH

In a round bottom flask, mPEG-COOH (500 mg), DCC (35 mg) and NHS (20 mg) were added to 7.5 mL of anhydrous DMF. The mixture was stirred for 2 h under nitrogen protection. Then, GPLGVRGDG peptide (140 mg) in anhydrous DMF (3 mL) was slowly added using a constant pressure dropping funnel. After stirring for 24 h at room temperature, the mixture was purified by dialysis (MWCO = 3500 Da) for 48 h, and lyophilized to a powder.

1.4 Synthesis of CPT-SS-OH

CPT (300 mg), DMAP (337 mg) and BTC (95 mg) were added to 20 mL of anhydrous DCM under nitrogen protection. After stirring at room temperature for 30 min, 2-

hydroxyethyl disulfide (664 mg) in anhydrous THF (3 mL) was slowly added and stirred overnight at room temperature in the dark. The mixture was respectively washed with 1M HCl, brine and water for three times. Then, the organic layer was dried with anhydrous sodium sulfate and filtered. The solution was removed by a vacuum rotary evaporator, and the crude product was purified by silica gel column chromatography to obtain the light yellow solid.

1.5 Synthesis of mPEG-pep-etcSS-CPT [3-4]

CPT-SS-OH (76 mg), mPEG-GPLGVRGDG-COOH (500 mg) and DMAP (14 mg) were dissolved in anhydrous DCM (12 mL). Next, DCC (32 mg) in anhydrous DCM was slowly added. Under nitrogen protection, the mixture was stirred at room temperature for 24 h in the dark. After the reaction was completed, the reaction solution was filtered to remove insoluble by-products and then added into a dialysis bag (MWCO = 3500 Da) to dialyze against distilled water for 48 h. A white solid was obtained after lyophilization.

1.6 Preparation of CPT-Loaded nanoparticles

The CPT-loaded mPEG-pep-etcSS-CPT nanoparticles were prepared by the film hydration method. Briefly, 6 mg of mPEG-pep-etcSS-CPT and 0.2 mg of CPT were dissolved in 4 mL of chloroform. The organic solvent was removed by vacuum rotary evaporator to form a uniform film on the wall of the bottle, and then 15 mL of deionized water was added to the bottle. The mixture was dispersed by ultrasonic for 3 min, and stirred for 3-4 h in the dark. At last, mPEG-pep-etcSS-CPT nanoparticles (P-PSC) were filtrated through 0.45 μm filter membrane and lyophilized. According to the similar procedure, mPEG-Pep-CPT nanoparticles (P-PC) and mPEG-etcSS-CPT nanoparticles (P-SC) were also prepared.

The amount of CPT in P-PSC was quantified via UV−vis spectroscopy based on the standard curve of CPT at λ =365 nm. Drug loading content (DLC) and drug loading efficiency (DLE) were calculated according to the literature. [5]

1.7 Material Characterization

^{1}H nuclear magnetic resonance (^{1}H NMR) spectra were collected using a Bruker 400 M apparatus. The solvents were $CDCl_3$ and DMSO-d_6, and the internal reference was tetramethylsilane (TMS). Molecular weights and polydispersity index of the mPEG-pep-etcSS-CPT were measured by a gel-permeation chromatograph (GPC) with Waters 1525 pump. The eluent used was THF, and the flow rate was 1.0 mL/min at 35 °C. Fourier transform infrared spectroscopy (FT-IR) was analyzed on a Bruker TENSOR

37 spectrometer through mixing lyophilized dry powder of the obtained mPEG-pep-etcSS-CPT with KBr and pressing it to a plate. The size, size distribution and zeta potential of micellar P-PSC in aqueous solution were measured by DLS (Nano ZS, Malvern). The morphology of the P-PSC micelle was characterized by transmission electron microscopy (TEM; Talos L120C G2, FEI).

1.8 Critical Micelle Concentration

Pyrene was used as the fluorescence probe to investigate the CMC of mPEG-pep-etcSS-CPT amphiphile. [6] The mPEG-pep-etcSS-CPT polymer was dispersed into solutions of different concentrations from 6×10^{-6} mg/mL to 0.2 mg/mL, where the final concentration of pyrene was 6×10^{-7} mol/L. The samples were equilibrated in the dark at room temperature for 24 h, to completely encapsulate the pyrene in micelles. The excitation spectra were recorded by a fluorescence spectrophotometer (F-4600, Hitachi) in the wavelength range of 300 to 380 nm. The emission wavelength was set at 390 nm. Finally, the intensity ratios (I_{342}/I_{339}) were plotted versus the logarithm of the polymer concentrations.

1.9 *In Vitro* Stability and Dual-Responsive Behaviors of P-PSC

The stability of CPT-loaded P-PSC was evaluated by DLS. The freeze-dried powder of P-PSC micelle was dispersed in PBS (pH 7.4), and stored at 4°C in the dark. At each given time point (0, 1, 2, 3, 4, 5, 6, 7 days), the change in particle size of P-PSC micelles with time was detected and analyzed.

The size changes of P-PSC micelle in response to MMP-2 and reduction conditions were also monitored by DLS measurements. Equal amounts of P-PSC micelle solution (1 mg/mL) was incubated with MMP-2 (100 μL) or GSH (10 mM) at 37°C. At predetermined time intervals, samples were taken for DLS measurements.

1.10 *In Vitro* Release of CPT

3 mL of CPT-loaded micelle PBS solutions were loaded in a dialysis bag (MWCO = 3500 Da), and dialyzed against 40 mL of corresponding buffer solution. Four different medium conditions were (i) PBS (pH 7.4), (ii) PBS (pH 7.4) containing 100 μL MMP-2, (iii) PBS (pH 7.4) containing 10 mM GSH, (iv) PBS (pH 7.4) containing 100 μL MMP-2 and 10 mM GSH. At predetermined time points, withdraw 1 mL of release medium for analysis of CPT concentrations and replenish with the same amount of fresh buffer. The cumulative release of CPT was determined by UV−vis spectrometer at 365 nm with the assistance of a standard curve.

1.11 *In Vitro* Cytotoxicity Assays

A549 cells and HepG2 cells were selected for cytotoxicity assays. A549 cells were cultured in 96 well plates in 100 μL of 1640 medium containing 10% FBS at 37°C under humidified CO_2 atmosphere (5%) for 24 h. Next, the medium was replaced with 100 μL of fresh 1640 medium containing 10% FBS, and various doses of free CPT, P-SC, P-PC, P-PSC or medium only (negative control) were added, and incubated for 48 h. All samples were prepared in triplicate. 20 μL volume of MTT labeling reagent was added to each well and incubated at 37 °C in the dark for 4 h. The medium was aspirated completely, and DMSO (150 μL) was added to dissolve the formed purple formazan crystals. Absorbance was measured at 570 nm and cell viability (%) was represented as the absorbance ratio of the test and negative control solutions. The cytotoxicity of free CPT, P-SC, P-PC and P-PSC against HepG2 was also determined by the same protocol.

1.12 Cell Apoptosis Analysis

The flow cytometry was performed to estimate the apoptosis-inducing capabilities of the P-PSC micelle. A549 cells were seeded into a 12-well plate and cultured overnight. Subsequently, cells were treated with appropriate amounts of free CPT, P-SC, P-PC and P-PSC (3.5 μg/mL CPT equivalents), and the untreated cells were set as negative controls. After incubation for 48 h, the cells were collected by trypsinization and centrifuged at 5000 rpm for 3 min. The cell apoptosis was further quantified by a flow cytometer (LSR Fortessa, BD) using Annexin V/PI test kit.

1.13 *In Vitro* Cellular Uptake.

CLSM (LSM 800 with Airyscan) was used to detect cellular uptake of free CPT and P-PSC micelle by A549 cells *in vitro*. Cells were seeded onto confocal dishes and cultured for 24 h. Then, free CPT, P-SC, P-PC and P-PSC (3.5 μg/mL CPT equivalents) were added and incubated for 1, 3, or 5 h. Afterward, the medium in the dishes was removed, and the cells were washed with PBS three times. The cells were fixed with 4% paraformaldehyde for 20 min and finally washed with cold PBS three times. At last, the cells were used for CLSM detection.

To study the RGD-responsiveness of P-PSC micelle, A549 cells in confocal dishes were pre-cultured with free RGD for 12 h. Cells without pretreatment were used as controls. After that, P-PSC micelles were then added and incubated for 3 h. Cells were washed with cold PBS for three times and fixed with 4% paraformaldehyde for 20 min, and finally washed with cold PBS for three times. The fluorescence images were collected using CLSM.

Flow cytometry measurements were carried out as follows. The cells were seeded in 12-well plates. After incubation with free CPT, P-SC, P-PC and P-PSC for 1, 3, or 5 h, the cells were collected by trypsinization and centrifuged at 5000 rpm for 3 min. Finally, the cells were suspended in PBS and analyzed for fluorescence intensity with the flow cytometer. The experimental approach to investigate the RGD-responsiveness of P-PSC micelles was similar.

1.14 *In Vivo* Antitumor Activity

4T1 cells were suspended in PBS (1×10^6 cells/mL) and transplanted into the BALB/c mice. Treatments were initiated when the tumor volume reached 100 mm^3. The mice were randomly divided into five groups (n=5). PBS, free CPT, P-SC, P-PC or P-PSC micelle was injected via the lateral vein at 2-day intervals at a dosage of 3 mg CPT/kg body weight. The tumor volumes were measured by a caliper every 2 days, and the body weights of mice were recorded. After observation for 16 days, the mice were sacrificed and tumors and major organs (heart, liver, spleen, lung, and kidney) were harvested for H&E assay and Ki67 immunohistochemical analysis.

1.15 Biodistribution and *in vivo* Imaging

The biodistribution was studied in 4 T1 tumor-bearing mice treated as above mentioned. Rhodamine B loaded mPEG-pep-etcSS-CPT nanoparticles were prepared by mixing mPEG-pep-etcSS-CPT (6 mg) and Rhodamine B (0.2 mg) by stirring at room temperature for 3 h in the dark. The resulted mPEG-pep-etcSS-CPT/RhB nanoparticles were filtrated through 0.45 μm filter membrane. The mice were intravenously injected with free RhB or mPEG-pep-etcSS-CPT/RhB nanoparticles (100 μL) and photographed using the In Vivo Imaging System (IVIS Spectrum, PerkinElmer, USA) with fluorescent filter sets (excitation/emission, 535/580) at 0, 4, 8, and 12 h. After 12 h injection, the mice were sacrificed, and the organs of liver, spleen, kidney, lung, heart, muscle, brain, intestines, and tumor were excised, washed with PBS. Their *ex vivo* images were also photographed using the same settings.

1.16 Ethics

All animal studies were carried out in conformity with the guidelines set by the Tianjin Committee of Use and Care of Laboratory Animals and the overall project protocols were approved by the Animal Experiments Ethical Committee of Nankai University.

2. Supplementary Figures

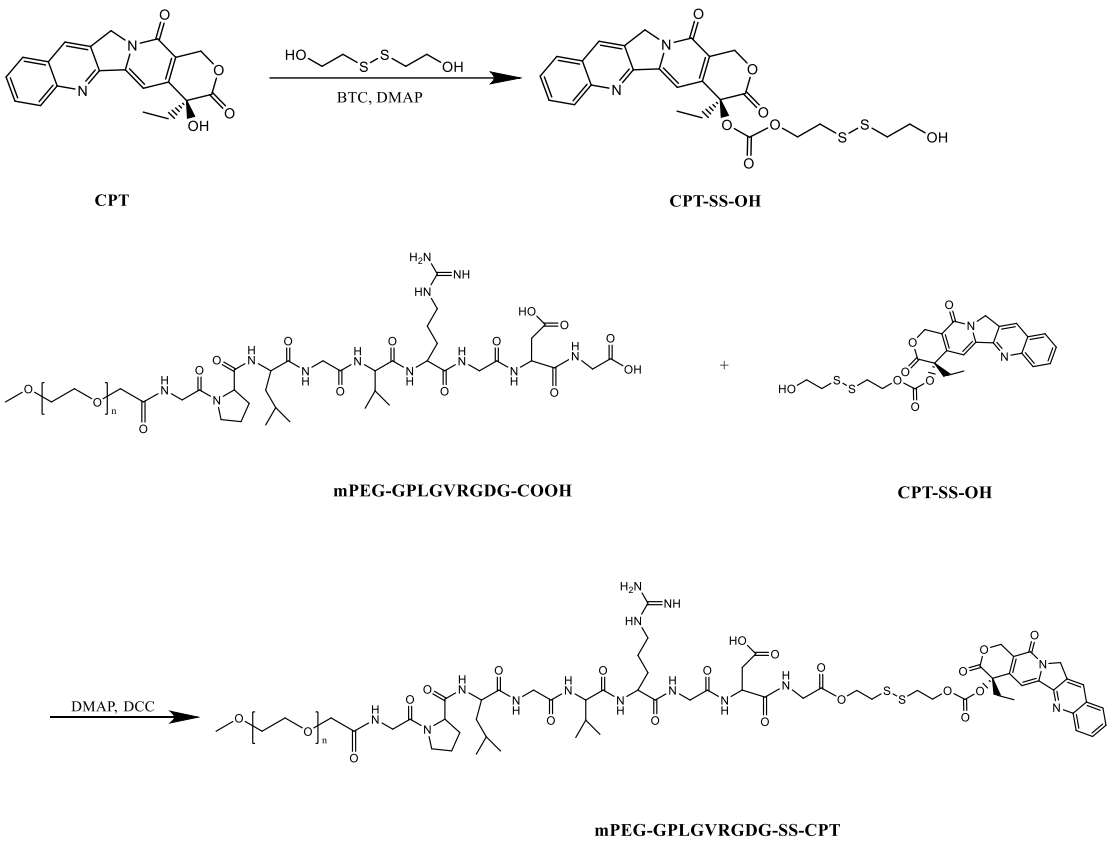

Fig. S1. Synthetic routes of CPT-SS-OH and mPEG-pep-etcSS-CPT.

(A)

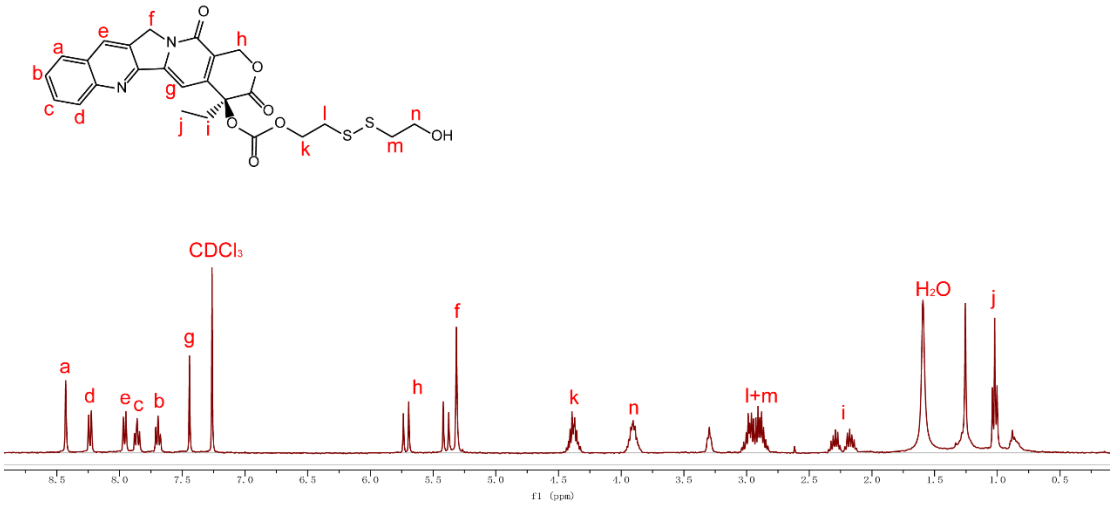

^{1}H NMR (400 MHz, Chloroform-*d*)：δ 8.43 (s, 1H), 8.24 (d, *J* = 8.6 Hz, 1H), 7.96 (d, *J* = 8.2 Hz, 1H), 7.90 – 7.82 (m, 1H), 7.69 (t, *J* = 7.6 Hz, 1H), 7.44 (s, 1H), 5.72 (d, *J* = 17.3 Hz, 1H), 5.40 (d, *J* = 17.3 Hz, 1H), 5.31 (s, 2H), 4.46 – 4.30 (m, 2H), 3.91 (dq, *J* = 12.6, 5.9 Hz, 2H), 2.93 (ddt, *J* = 31.7, 19.3, 6.5 Hz, 4H), 2.23 (ddq, *J* = 52.2, 14.7, 7.5 Hz, 2H), 1.02 (t, *J* = 7.5 Hz, 3H).

(B)

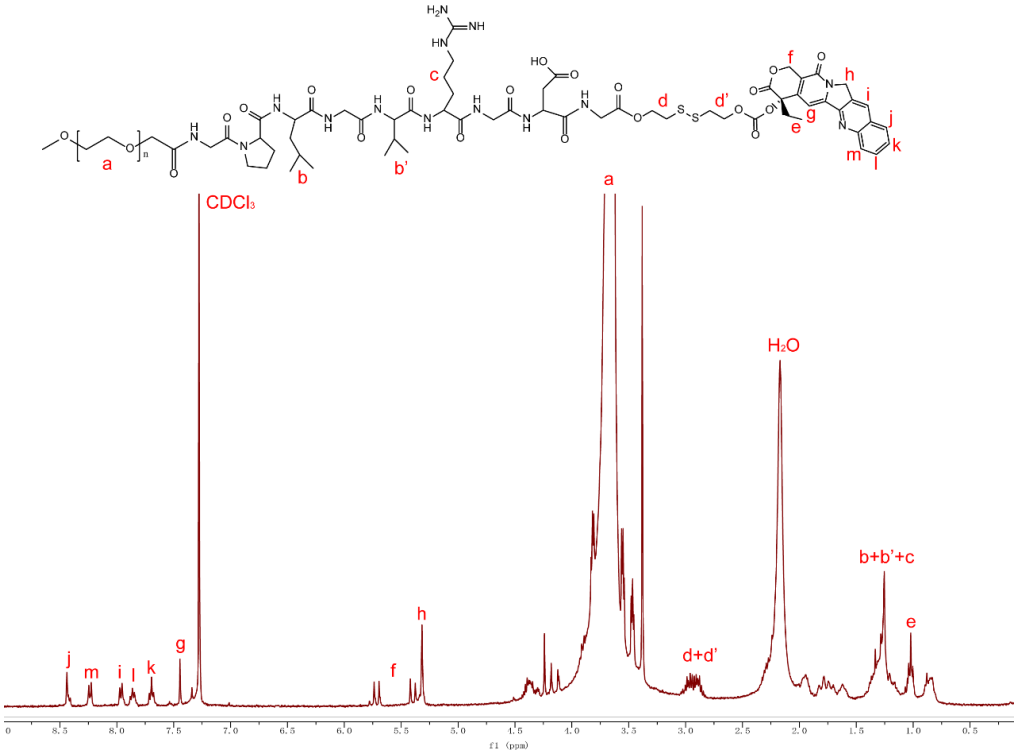

Fig. S2. ^{1}H NMR spectra of (A) CPT-SS-OH and (B) mPEG-pep-etcSS-CPT in $CDCl_3$.

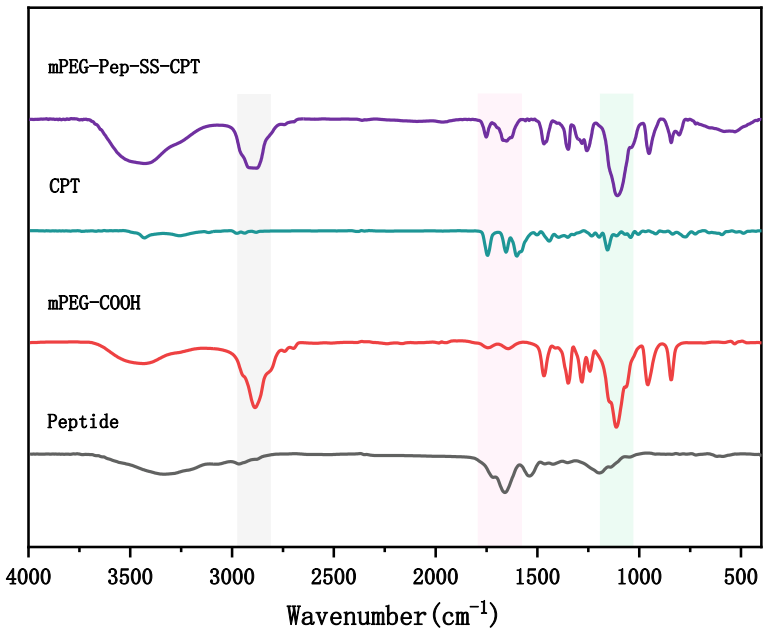

Fig. S3. FT-IR spectra of mPEG-pep-etcSS-CPT, CPT, mPEG-COOH and peptide.

Table S1 GCP data of the prepared mPEG-pep-etcSS-CPT.

Samples	Mn （Daltons）	Mw （Daltons）	Polydispersity
mPEG-pep-etcSS-CPT	5228	5348	1.0229

Table S2 Characterization of the prepared mPEG-pep-etcSS-CPT micelles comparing with literature data.

Micelle systems for CPT	Drug loading efficiency (DLE)	CMC (μg/mL)	Cumulative release (24 h) in presence of GSH	literature
CPT–SS–CPT-loaded PCL–PEG–PCL micelles	63.33%	--	--	[7]
CFS@PF/CPT nanoassembly	46.42%	--	62.41%	[8]
(mPEG–PCL)-loaded CPT-Mal-CPT nanoparticles	56%	--	60%	[9]
CPT-S-S-PEG-iRGD@IR780 micelles	--	0.46	55%	[10]
PEGHC micelles	49.5%	34.5	85%	[11]
TL-CPT NPs	22.4%	--	60%	[12]
PLGA-PEI/CPT micelles	8.3%	--	61%	[13]
mPEG-pep-etcSS-CPT micelles	67.7%	0.2	81%	This work

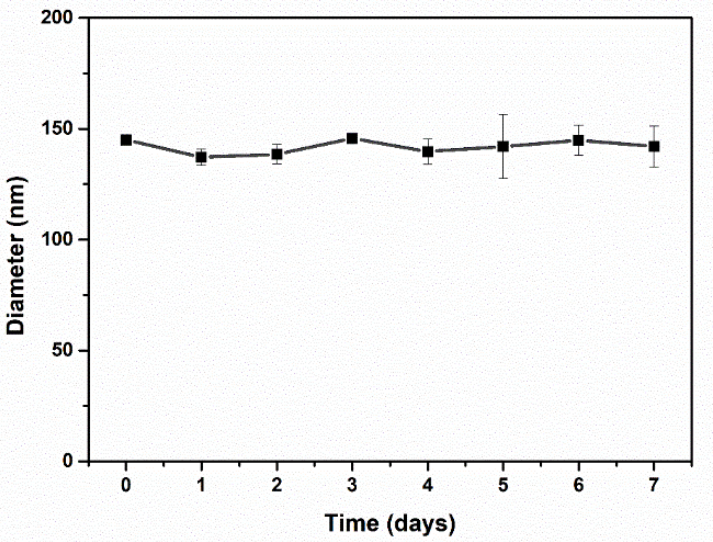

Fig. S4 The variation of the particle size of P-PSC with time.

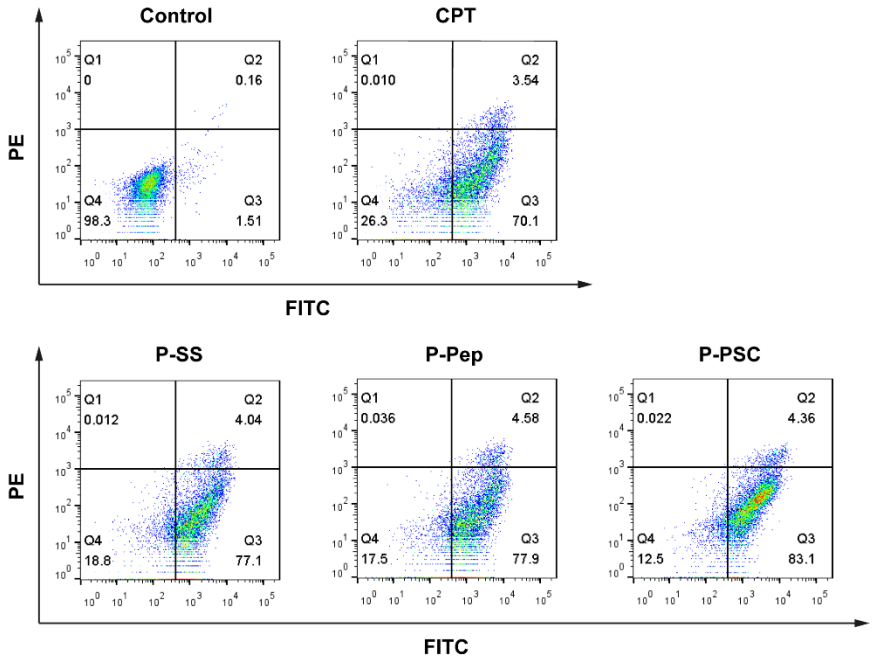

Fig. S5. Apoptotic analysis of A549 cells determined by flow cytometry. Four distinct phenotypes: viable cells (lower left quadrant); early apoptotic cells (lower right quadrant); late apoptotic cells (upper right quadrant); necrotic or dead cells (upper left quadrant).

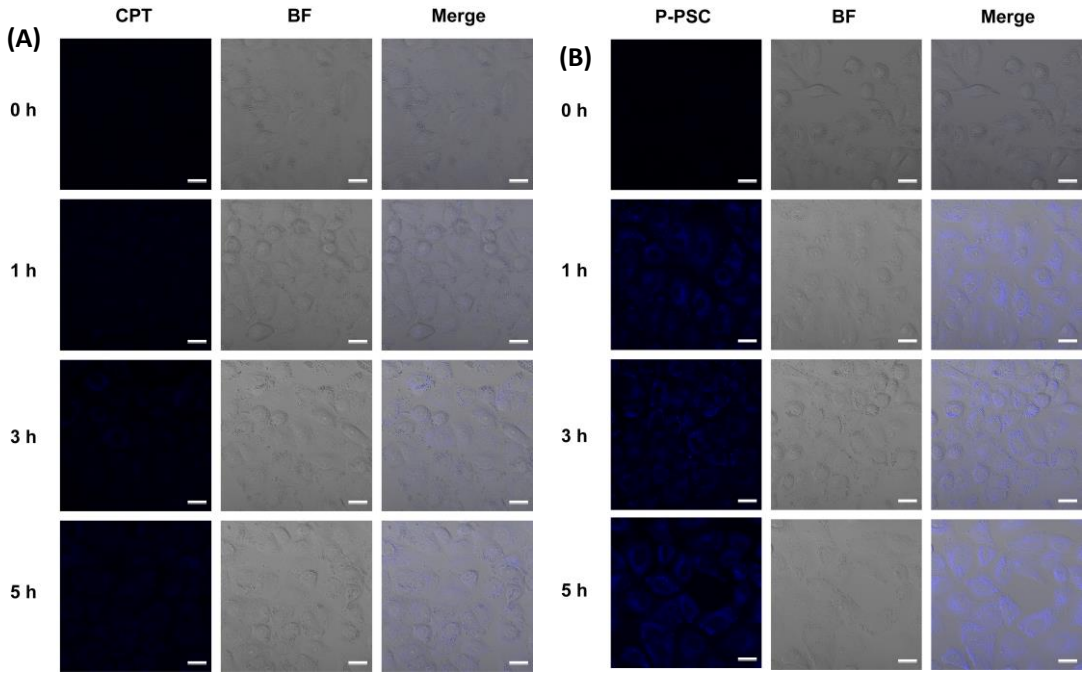

Fig. S6. Confocal microscopy images of A549 cells incubated with CPT (A) and P-PSC (B) for 1, 3 and 5 h. Scale bars = 20 μm.

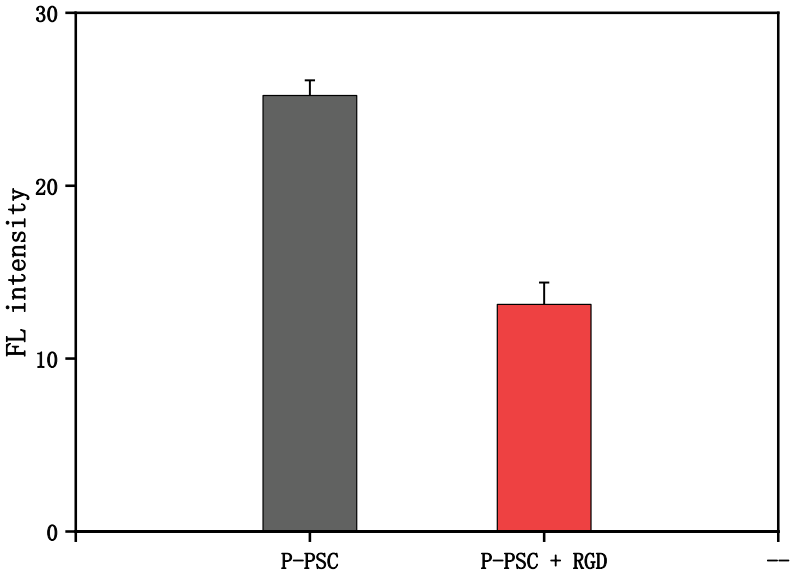

Fig. S7. Comparison of mean fluorescence intensity of A549 cells incubated with P-PSC in the absence or presence of free RGD.

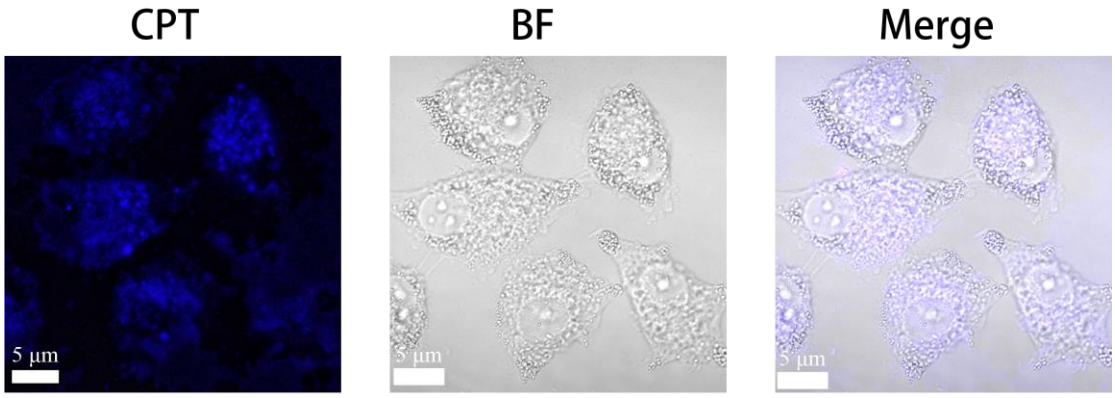

Fig. S8. Confocal microscopy images of A549 cells incubated with P-PSC for 5 h demonstrating increased blue fluorescence from CPT in the cell nuclei which indicated the breakage of disulfide bond intracellularly by the endogenous GSH.[14]

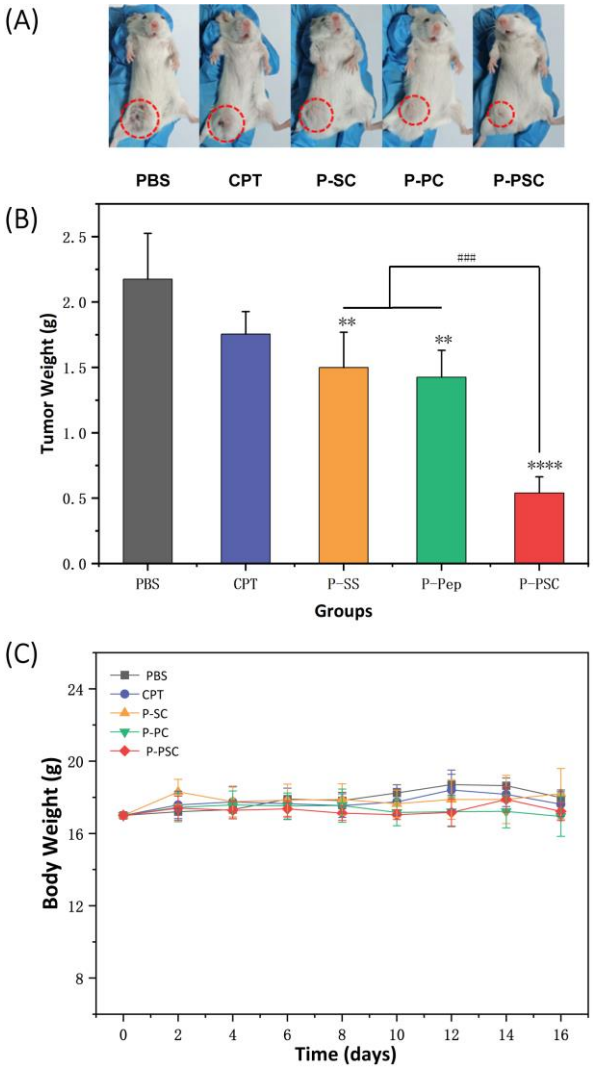

Fig. S9. *In vivo* antitumor efficacy. (A) Photographs of solid tumors in different groups at the end of treatment, (B) Tumor weight of different groups, (C) body weight changes in different groups, ****P < 0.0001, **P < 0.01, compared to the PBS group; $^{###}$P < 0.001 compared to the P-PSC group.

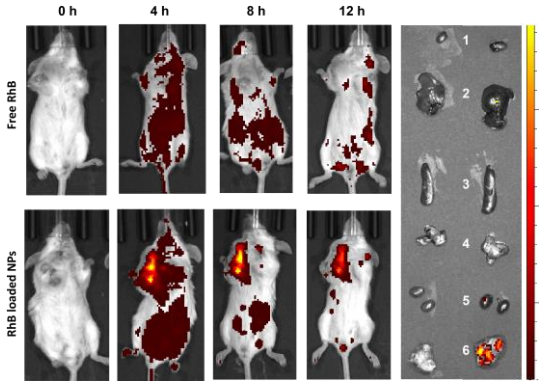

Fig. S10. Fluorescence images of mice and tissues after i.v. injection of the free RhB or mPEG-pep-etcSS-CPT/RhB nanoparticles (1, heart; 2, liver; 3, spleen; 4, lung; 5, kidney; 6, tumor).

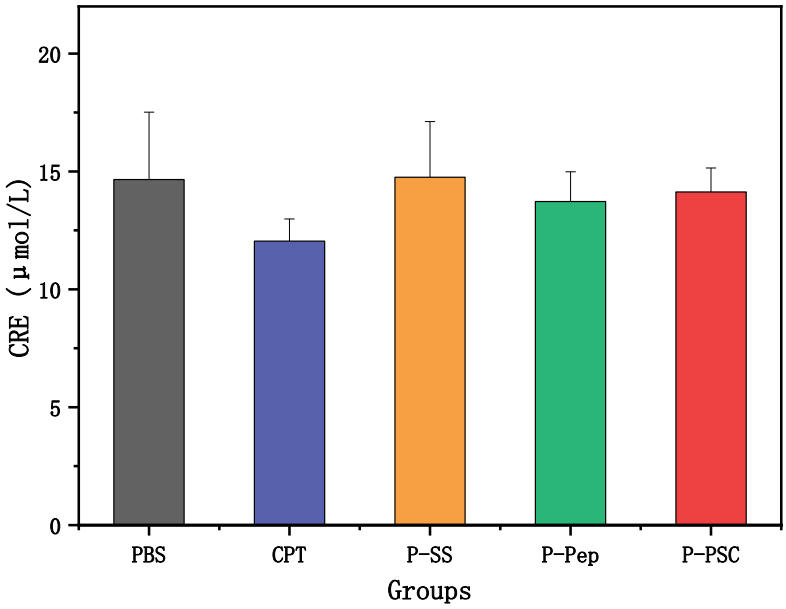

Fig. S11. Creatine (CRE) measurements in the serum of each group of mice at the end of treatment.

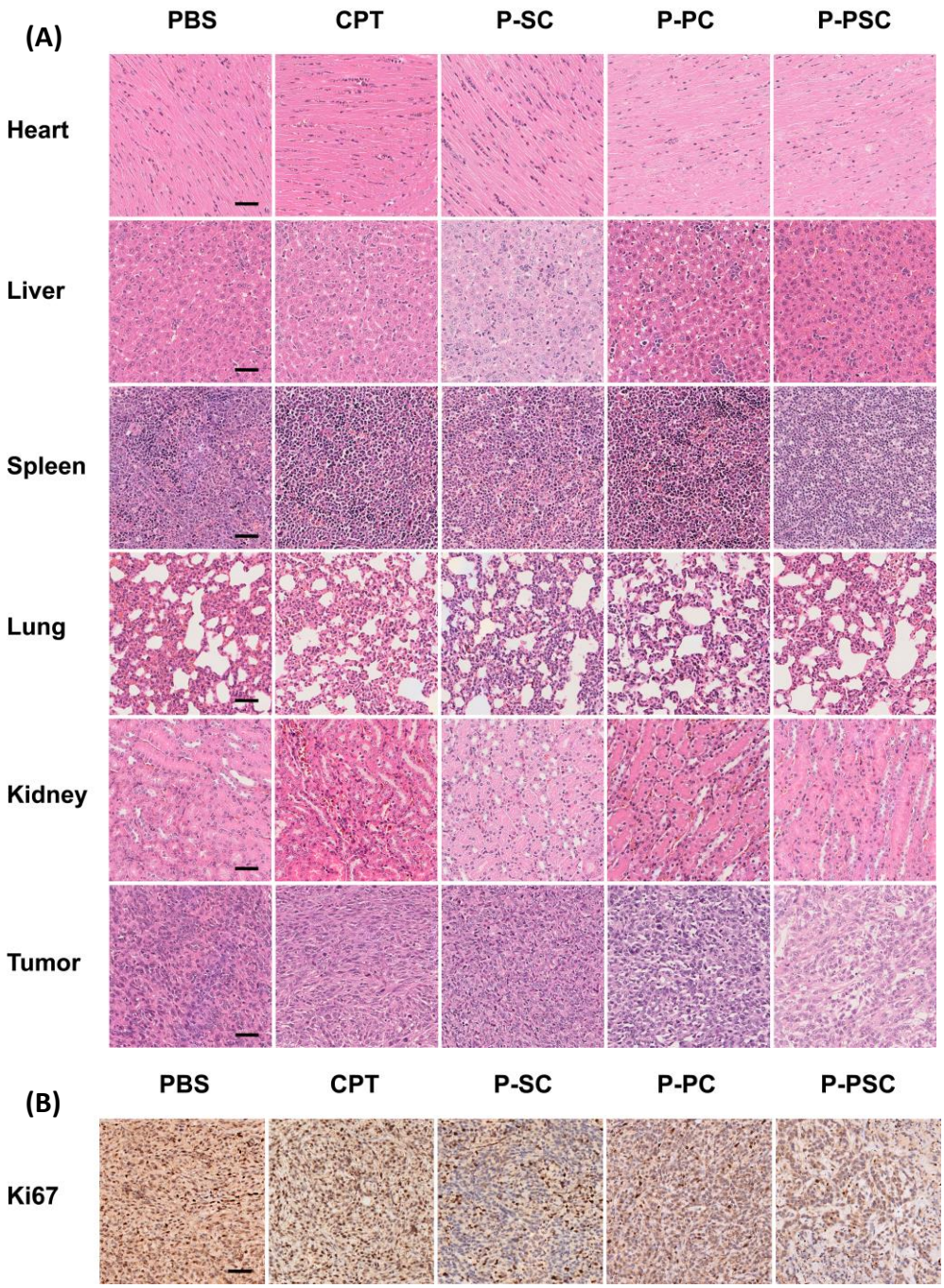

Fig. S12. (A) H&E staining of main organs (heart, liver, spleen, lung, kidney) and tumor tissue. (B) Ki67 staining of tumor tissue (scale bar = 50 μm).

Reference

[1] Du J, Lane L A, Nie S. Stimuli-responsive nanoparticles for targeting the tumor microenvironment[J]. Journal of Controlled Release, 2015, 219: 205-214.

[2] Zhang J, Yuan Z F, Wang Y, et al. Multifunctional envelope-type mesoporous silica nanoparticles for tumor-triggered targeting drug delivery[J]. Journal of the American Chemical Society, 2013, 135(13): 5068-5073.

[3] Jain A K, Gund M G, Desai D C, et al. Mutual prodrugs containing bio-cleavable and drug releasable disulfide linkers[J]. Bioorganic Chemistry, 2013, 49: 40-48.

[4] Tan X, Lu X, Jia F, et al. Blurring the role of oligonucleotides: spherical nucleic acids as a drug delivery vehicle[J]. Journal of the American Chemical Society, 2016, 138(34): 10834-10837.

[5] Lv S, Wu Y, Cai K, et al. High drug loading and sub-quantitative loading efficiency of polymeric micelles driven by donor–receptor coordination interactions[J]. Journal of the American Chemical Society, 2018, 140(4): 1235-1238.

[6] Ray G B, Chakraborty I, Moulik S P. Pyrene absorption can be a convenient method for probing critical micellar concentration (cmc) and indexing micellar polarity[J]. Journal of colloid and interface science, 2006, 294(1): 248-254.

[7] Yu B, Meng Q, Hu H, et al. Construction of dimeric drug-loaded polymeric micelles with high loading efficiency for cancer therapy[J]. International Journal of Molecular Sciences, 2019, 20(8): 1961.

[8] Direrse W B, Getachew G, Hsiao C H, et al. Surface-engineered CuFeS2/Camptothecin nanoassembly with enhanced chemodynamic therapy via GSH depletion for synergistic photo/chemotherapy of cancer[J]. Materials Today Chemistry, 2022, 26: 101158.

[9] Chi Y, Wang Z, Wang J, et al. Dimeric camptothecin-loaded mPEG-PCL nanoparticles with high drug loading and reduction-responsive drug release[J]. Colloid and Polymer Science, 2020, 298(1): 51-58.

[10] Lu L, Zhao X, Fu T, et al. An iRGD-conjugated prodrug micelle with blood-brain-barrier penetrability for anti-glioma therapy[J]. Biomaterials, 2020, 230: 119666.

[11] Li D, Liang Y, Lai Y, et al. Polymeric micelles with small lipophilic moieties for drug delivery[J]. Colloids and Surfaces B: Biointerfaces, 2014, 116: 627-632.

[12] Li J, Hu Z E, Yang X L, et al. Hierarchical targeted delivery of lonidamine and camptothecin based on the ultra-rapid pH/GSH response nanoparticles for synergistic chemotherapy[J]. ACS Applied Bio Materials, 2020, 3(11): 7382-7387.

[13] Hao X, Gai W, Wang L, et al. 5-Boronopicolinic acid-functionalized polymeric nanoparticles for targeting drug delivery and enhanced tumor therapy[J]. Materials Science and Engineering: C, 2021, 119: 111553.

[14] Zhang F, Zhu G, Jacobson O, et al. Transformative nanomedicine of an amphiphilic camptothecin prodrug for long circulation and high tumor uptake in cancer therapy[J]. Acs Nano, 2017, 11(9): 8838-8848.